Runoff sensitivity to climate and land-use changes: A case study in the Longtan basin, Southwestern China

Guiyan Mo, Ya Huang, Qing Yang, Dayang Wang and Chongxun Mo

ABSTRACT

Based on the scenario hypothesis method, this paper applied a Soil and Water Assessment Tool (SWAT) to analyze the sensitivity of runoff to climate and land-use changes in the Longtan basin, China. Results indicated that (1) for every 1 °C increase in temperature, the average annual runoff decreased by 9.9 mm, and the average annual evaporation increased by 9.3 mm. However, for every 10% increase in rainfall, the average annual runoff and evapotranspiration increased by 96.3 mm and 11.53 mm, respectively. Obviously, runoff was more sensitive to the change in rainfall than temperature in the Longtan basin. Meanwhile, (2) forestland could conserve water resources, but its water consumption was larger. Although grassland played a relatively small role in water conservation, it consumed less water. At the same time, increasing the area of forestland and grassland could weaken peak floods, and the water retention function of vegetation could prevent runoff from increasing and decreasing steeply. Therefore, it is worth improving vegetation coverage.

Key words | climate change, land-use change, Longtan basin, sensitivity, SWAT model

Guiyan Mo (corresponding author)
College of Computer and Information,
Hohai University,
Nanjing 211100,
China
E-mail: *guiyan.mo@hotmail.com*

Guiyan Mo
Ya Huang
Qing Yang
Chongxun Mo
College of Civil and Architectural Engineering,
Guangxi University,
Nanning 530004,
PR China

Ya Huang
State Key Laboratory of Simulation and Regulation of Water Cycle in River Catchment,
China Institute of Water Resources and Hydropower Research,
Beijing 100038,
China

Dayang Wang
School of Geography and Planning,
Sun Yat-sen University,
Guangzhou 510275,
China

HIGHLIGHTS

- Constructing 25 climate change scenarios based on CMIP5 simulation results and local temporal and spatial variation characteristics.
- Constructing 4 land-use scenarios based on its variation characteristics and local development plan.
- Simulating and quantifying runoff response to different climate and land-use change scenarios.
- Identifying the major impact factors for runoff variability.
- Experiment in the karstic basin, where there is a lack of related research.

INTRODUCTION

Under changing environments, the water cycling process and its formation characteristics are increasingly sensitive to the changes in global climate and human activities (Chenoweth *et al.* 2011). Atmospheric warming intensives the movement of water molecules as well as the movement of evaporation, rainfall and soil moisture. Finally, it affects the spatial and temporal distribution of water resources (Şen 2009). On the other hand, human activities affect the process of infiltration, soil moisture, and surface runoff, based on the variation in land-use patterns (Green *et al.* 2007). Differences between water cycle processes and water resource allocation caused by climate change and human activities are prone to induce the problems of extreme hydrometeorological events (droughts and floods) and water pollution (Wu & Tan 2012). Therefore, related subjects and studies of climate change (at regional or global scales) and the changes in water resources have become issues of increasing concern to experts

doi: 10.2166/wcc.2020.196

and scholars in recent years (Chen *et al.* 2012; Dittmer 2013; Kim *et al.* 2014; Jiang *et al.* 2015; Zhou *et al.* 2015; Wu *et al.* 2017; Gusev *et al.* 2018; Yan *et al.* 2019).

Longtan River basin, located in the upper reaches of the Hongshuihe River, is the main stream of the Xijiang River in the Pear River system, China. After the construction and operation of the Longtan hydropower dam, regional climate has changed. Similarly, Miller (2005) noticed that reservoir area will influence the patterns of rainfall, wind, and temperature and found that the change from a natural river channel to a reservoir around the Three Gorges Dam decreases upward motion. Also, it further increases evaporation and surface temperature, cools the lower atmosphere, and increases rainfall as well as sinking air mass. Similar changes are shown in the study area. At the same time, with the change in vegetation coverage during the construction of the Longtan hydropower dam (2001), some changes occurred in the hydrological circulation process and water environment in the upper reaches (Green *et al.* 2007). Meanwhile, according to the existing measured runoff data, the study basin has been in a state of long-term runoff decline (2001–2010) (Huang *et al.* 2017). Therefore, future water resources will face many uncertainties (e.g., randomness, fuzziness, gray), and new challenges will arise for the sustainability and management of water resources as well as socioeconomic development in the study catchment. However, runoff-sensitivity research in the study catchment is scarce, although watershed managers indeed call for such study.

Based on the above-mentioned analysis, this paper focused on sensitivity analysis of runoff to climate and land-use changes, and tried to identify the major impact factors for runoff variability in this basin. The goal was implemented through a combination of the Soil and Water Assessment Tool (SWAT) model and the research approach of 'climate scenarios-hydrological simulation-response analysis'. First, temperature and rainfall were selected as the main influencing factors according to the related researches (Huang *et al.* 2017; Mo 2018). Second, a satisfactory SWAT model was set up to simulate the hydrological process under different scenarios of climate and land-use change. Finally, the sensitivity of runoff to climate and land-use changes in the Longtan basin was quantified. The purpose of this paper was to further understand the influence mechanism of runoff variations, and provide a scientific basis for the possible subsequent challenges brought by climate change and changes in land-use patterns in the future. In general, the result of this paper can help policymakers and planners to propose suitable management practices, which can cope with the quantitative impacts of climate and land-use changes on runoff in this basin or other similar catchments.

STUDY AREA

The Longtan watershed, which is a leading reservoir of southwestern China, was selected as the study site for sensitivity analysis of runoff to climate and land-use changes. This catchment stretches from latitudes of 23°11′–27°01′N and longitudes of 102°14′–107°32′E, and extends across an area of 98,500 km^2 around Yunnan Province, Guizhou Province, and Guangxi Zhuang Autonomous Region (Figure 1). Tian-e hydrologic station is the outlet to the Longtan reservoir, which can be used not only for hydropower generation but also for water supply and flood control (Shi 2014). The average elevation of the Longtan basin is 1,450 m, with a valley elevation of 23 m in the southeast region and a plateau with an elevation of 3,358 m in the northwest area.

The climate of this catchment is sub-subtropical with a hot-wet summer season and cold-dry winter season. The average annual temperature for 1959 to 2013 ranges from 12.3 °C to 21.3 °C and the mean annual rainfall increases from 760 mm in the western region to 1,860 mm in the eastern area, where flood season rainfall (April to October) accounts for 89% of the annual precipitation. The main land uses of the study area are forestland and grassland, with 34.83% vegetation cover. The soil texture of loam accounts for 60% of the soil types.

METHODS AND DATA

SWAT model and data preparation

The SWAT model, a semi-distributed and physically based model, was designed to predict the impact of land management practices on water, sediment, and agricultural

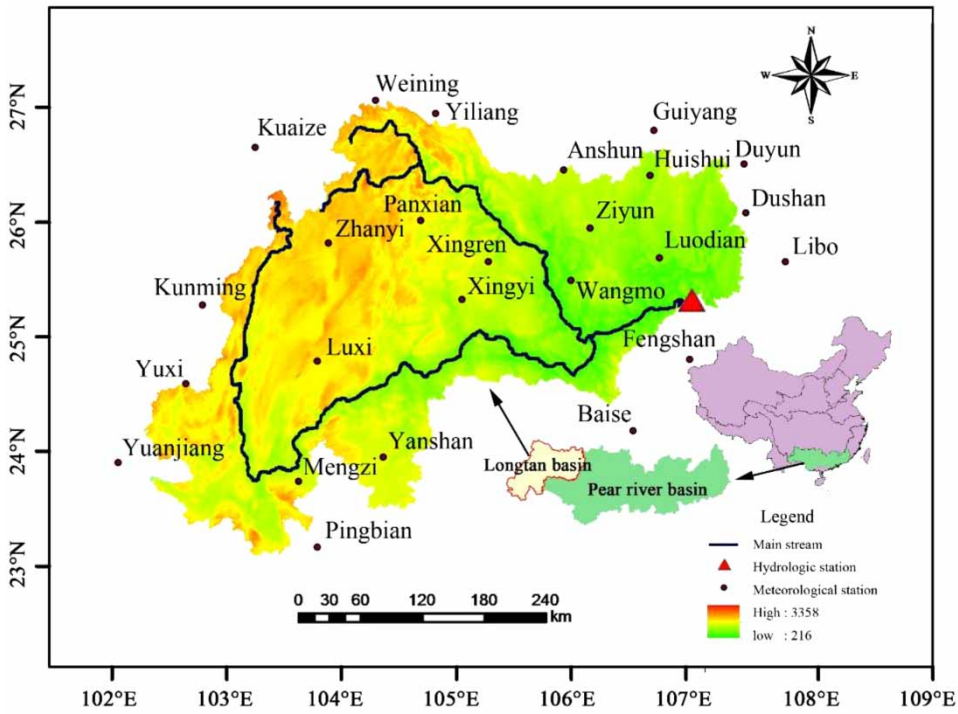

Figure 1 | Longtan basin (98,500 km^2), 25 meteorological stations and the Tian-e hydrologic station adopted for analysis.

chemical yields in large complex watersheds (Arnold 2012). The SWAT model divides a watershed into sub-basins and further subdivides each sub-basin into a number of hydrological response units (HRUs). Taking HRUs as the basic unit, hydrological components are simulated and aggregated for each sub-basin, and then routed to the basin outlet throughout the channel network to obtain the hydrological components based on water balance equation (Arnold *et al.* 1998). In this paper, SWAT was based on an interface of ArcGIS software, which provided an easy linkage of SWAT CUP for model calibration and uncertainty/sensitivity analysis (Abbaspour *et al.* 2007). Therefore, the required spatial data (digital elevation model (DEM), land-use, and soil type maps) and temporal data (meteorological data) were either raster or vector data sets.

DEM data for the Longtan watershed (Figure 1) was downloaded from the Geospatial Data Cloud website (http://www.gscloud.cn) and had a spatial resolution of 90 m. Land-use data in 2010 and soil map in 2000 were both provided by the Resource and Environment Data Cloud Platform of China (http://www.resdc.cn) and had a resolution of 1:1,000,000. At the same time, the reclassified land-use types of forest (main land use type), grassland, water body, urban area, bare land, paddy, and cultivated land were assigned as FRST, PAST, WATR, URBN, BALD, PADY, and AGRL, respectively (Wang *et al.* 2014). Meanwhile, the 35 different soil types were reclassified into seven soil types in the study catchment according to the FAO classification (Chesworth *et al.* 2008). These soils were Haplic Alisols (40.74%), Chromic Cambisols (31.03%), Humic Acrisols (15.44%), Dystric Cambisols (5.39%), Rendzic Leptosols (4.82%), Cumulic Anthrosols (2.28%), and Ferric Lixisols (0.30%).

Daily average, maximum and minimum temperatures, wind speed, relative humidity and precipitation data for the 25 meteorological stations (Figure 1) were obtained from the China Meteorological Data Sharing Service System (http://data.cma.cn) and met the requirements of data quality control, consistency check and record correction and recheck, covering the 55-year period from 1959 to 2013. Solar radiation data were simulated via the weather generator and other obtained climate data. Meanwhile, for the missing climate data at some stations over a short time, this paper used ArcGIS software to consider the correlation between meteorological stations for interpolation and

supplementation, in order to improve the simulation accuracy of the SWAT model (Liston & Elder 2006).

Streamflow data consisted of the measured inflow after dam construction and the runoff deduced from the near-by Tian-e hydrological station before dam construction. Runoff data from 1959 to 2013 could be used for model calibration and validation.

SWAT model calibration and validation

A SWAT model was set up for hydrological simulation in the Longtan basin based on data listed above. The study watershed was divided into 33 sub-basins and further discretized to 277 HRUs. Meanwhile, 13 parameters were chosen from the literature (Lv *et al.* 2014; Huang *et al.* 2018) to identify five sensitive parameters for model calibration (1985–1998) and validation (1999–2013), which are listed in Table 1. Meanwhile, Nash–Sutcliffe efficiency (NSE, Equation (1)) and coefficient of determination (R^2, Equation (2)) were used for evaluating the performance of the SWAT model in this study as recommended by Ghoraba (2015) and Moriasi *et al.* (2007):

$$NSE = 1 - \frac{\sum_{i=1}^{n} (Q_{obs,i} - Q_{sim,i})^2}{\sum_{i=1}^{n} (Q_{obs,i} - \bar{Q}_{obs})^2} \quad (1)$$

$$R^2 = \frac{\left[\sum_{i=1}^{n} (Q_{obs,i} - \bar{Q}_{obs})(Q_{sim,i} - \bar{Q}_{sim})\right]^2}{\sum_{i=1}^{n} (Q_{obs,i} - \bar{Q}_{obs})^2 \sum_{i=1}^{n} (Q_{sim,i} - \bar{Q}_{sim})^2} \quad (2)$$

where $Q_{obs,i}$ and $Q_{sim,i}$ are the observed and simulated discharge at time step i, respectively; $\bar{Q}_{obs}$ and $\bar{Q}_{sim}$ are the average observed and simulated discharge.

Climate change modeling scenarios

According to the previous studies by Mo (2018) and Huang *et al.* (2017), temperature and rainfall change rates were about 0.13 °C/10a and 23.2 mm/10a, respectively. Considering the possible extreme weather and the local weather conditions, a 20% change will occur in rainfall in the near future. Meanwhile, temperature variety was related to precipitation change based on CMIP5 simulation results (Zhou *et al.* 2014) and a 2 °C change was assumed for temperature, which fitted the temperature circumstances in the study area (Huang *et al.* 2017; Mo 2018). Finally, 25 climate change scenarios were constructed based on their temporal and spatial variation characteristics and the situation hypothesis method (Jones *et al.* 2006; Somura *et al.* 2009), illustrated as Table 2. It was further simulated in the SWAT model.

Variation percentage of annual runoff under climate change can be calculated by Equation (3) (Silberstein *et al.* 2012):

$$b = \frac{(y_i - y_0)}{y_0} * 100\% \quad (3)$$

where y_i is the average annual runoff generated by the ith climate change scenario, mm, and y_0 is the average annual runoff generated by the current climatic condition, mm.

Land-use change modeling scenarios

According to the measures of conversion of cropland to forest and grassland in western China by Li (2002) and corresponding change models by Li & Wu (2002), four land-use

Table 1 | Calibrated values of five sensitivity parameters in the SWAT model

Sensitivity ranking	Parameter	Description	Range	Fitted value	Calibration method
1	CN_2	SCS runoff curve number for moisture condition II	0.056–0.18	0.06	Replace
2	ALPHA_BF	Base-flow alpha factor	0.62–0.92	0.67	Added
3	GW_DELAY	Groundwater delay time (days)	52.08–161.58	98.79	Added
4	GWQMN	Threshold depth of water in the shallow aquifer required for return flow to occur	0.07–0.95	0.10	Aadded
5	GW_REVAP	Groundwater 'revap' coefficient	0.01–0.15	0.15	Aadded

Table 2 | Twenty-five climate change scenarios for sensitivity analysis

	Change rate of rainfall from baseline period/%				
Temperature variation/°C	**(−20)**	**(−10)**	**0**	**10**	**20**
−2	SS1	SS2	SS3	SS4	SS5
−1	SS6	SS7	SS8	SS9	SS10
0	SS11	SS12	SS13	SS14	SS15
1	SS16	SS17	SS18	SS19	SS20
2	SS21	SS22	SS23	SS24	SS25

Note: The first 'S' means sensitivity and the second 'S' represents scenarios.

type scenarios (SL1, SL2, SL3 and SL4) were set in this paper based on land-use data of 2010 (Supplementary material, Figure S1), topographic slope and vegetation types. Scenario 1 (SL1, 'S' means sensitivity, 'L' represents land-use type) assumed that all the current cultivated land would be converted to forestland and that the remaining land-use types would remain constant. In this situation, the forest coverage was 63%, and the grassland coverage rate was 26.69%. Scenario 2 (SL2) assumed that 14.29% of the current cultivated land would be changed to grassland, with 48.73% forest coverage and 40.96% grassland. Scenario 3 (SL3) assumed that all the current forestland would be converted to grassland for grazing and no forest land would remain. Scenario 4 (SL4) assumed that all the current grassland would be transformed to cultivated land, leaving no grassland in the Longtan basin. Simulation results of scenario 1 and scenario 2 reflect the hydrology response to regular policies of conversion of cropland to forest and grassland, and scenario 3 reflects the possible land-use change of overgrazing, which calls for a great demand for grassland. Scenario 4 demonstrates land-use varying from rangeland to bare ground, which is a common trend for farming in the study area.

Average monthly/annual runoff and the conservation index were evaluated in this paper. Meanwhile, different land-use scenarios represent different vegetations, and further have different effects of water conservation as well as climate regulation. For instance, forest not only consumed water resources but also improved air humidity. Fortunately, a measurement indicator of the conservation index can reflect the stability of hydrological processes and estimate the demand for water supply (Pizzolotto & Brandmayr 1996). The index can be measured by Equation (4):

$$\beta = \frac{Q_m}{Q_v} \tag{4}$$

where Q_m and Q_v are the streamflow in the driest month and the average annual flow, respectively, m^3/s.

RESULTS

The obtained coefficient of determination statistics R^2 (0.75 for annual calibration during 1987–1998, 0.88 for annual validation during 1999–2013) represent good consistency between the observed and simulated data and indicated low error variance. Furthermore, the NSE values were 0.85 for annual calibration and 0.88 for annual validation (Table 3). On the other hand, the calculated R^2 (0.94 for monthly calibration, 0.91 for monthly validation) and NSE (0.94 and 0.81) represented good matches between the monthly observed and simulated runoff (Figure 2) (Moriasi *et al.* 2007).

Sensitivity analysis under climate change

Variation in annual runoff

Runoff variability under different climate change scenarios (Table 4) showed that streamflow decreased when catchment rainfall decreased or temperature increased. Generally, for every 1 °C increase in the temperature of the basin, the average annual runoff decreased by 9.9 mm, and for every 10% increase in rainfall in this basin, the average annual runoff increased by an average of 96.3 mm.

Table 3 | Nash–Sutcliffe efficiency (NSE) and coefficient of determination (R^2) statistics for model calibration and validation periods

	Calibration from 1987 to 1998		Validation from 1999 to 2013	
Statistic	**Monthly**	**Yearly**	**Monthly**	**Yearly**
NSE	0.94	0.85	0.81	0.88
R^2	0.94	0.75	0.91	0.88

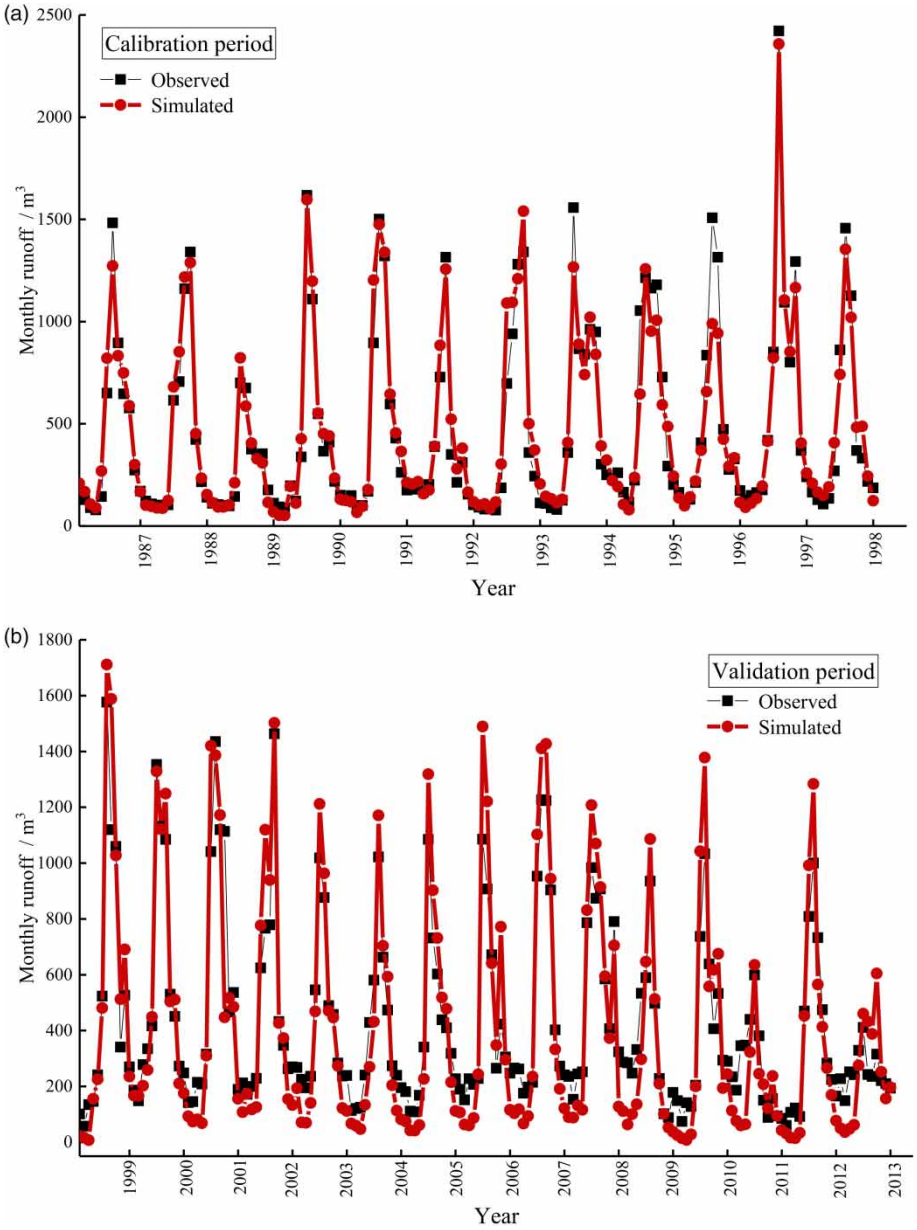

Figure 2 | Simulated and measured monthly runoff during the (a) calibration and (b) validation period.

Table 4 | Runoff variability under 25 climate change scenarios

		Rainfall/%				
Changing items	**Temperature/°C**	**(−20)**	**(−10)**	**0**	**10**	**20**
Runoff/mm	−2	−168.6	−75.5	20.9	119.8	220.1
	−1	−178.3	−85.6	10.5	109.0	209.1
	0	−187.5	−95.5	0.0	98.1	197.8
	1	−195.5	−104.2	−9.3	88.2	187.4
	2	−203.4	−112.9	−18.8	78.1	176.8

Specifically, from Table 4, the annual runoff decreased by 9.3 mm and 9.5 mm when the temperature increased by 1 °C and 2 °C, respectively. Correspondingly, decreases in temperature of 1 °C and 2 °C caused increases of 10.5 mm and 10.4 mm in streamflow, respectively, which were both based on the same rainfall. In contrast, mean annual runoff had a positive correlation with precipitation. Specifically, the increased scenarios for rainfall (10 and 20%), based on the same temperature, had induced streamflow increase of 98.1 mm and 99.7 mm, respectively, and runoff showed a decrease of 95.5 and 92 mm when rainfall was reduced by 10 and 20%, respectively. Obviously, runoff can be concluded to be more sensitive to the changes in rainfall than in temperature.

Variations in evaporation

Evaporation variations related to the changes in temperature and rainfall (Table 5) showed that, on the one hand, for every 1 °C increase in temperature, the average annual evaporation increased by 9.3 mm; on the other hand, for every 10% increase in rainfall, the mean annual evaporation increased by an average of 11.53 mm. Specifically, evaporation maintained the same change trend as temperature and increased by 8.6 and 9 mm, respectively, when the temperature increased by 1 °C and 2 °C, while evaporation decreased by 9.9 mm and 9.8 mm when the temperature decreased by 1 °C and 2 °C, respectively, based on the same rainfall conditions. Similar results can be observed for the changes in rainfall. Evaporation increased or decreased with the increase or decrease in precipitation (increased 9.9 mm and 8.3 mm for 10 and 20% increase in rainfall, decreased 12.4 mm and 15.5 mm for 10 and 20% decrease in rainfall, respectively). In view of these results, evaporation was more sensitive to the changes in rainfall than in temperature.

Sensitivity analysis under land-use change

The change amplitude of four land-use scenarios from the baseline period (2010) is shown in Table 6.

Table 5 | Evaporation variability under 25 climate change scenarios

		Rainfall/%				
Changing items	**Temperature/°C**	**(−20)**	**(−10)**	**0**	**10**	**20**
Evaporation/mm	−2	−45.6	−31.1	−19.7	−10.5	−2.8
	−1	−36.4	−21.7	−9.9	−0.4	7.6
	0	−27.9	−12.4	0	9.9	18.2
	1	−20.4	−4.2	8.6	19.1	28
	2	−13	4	17.6	28.7	38

Table 6 | Change amplitude of four land-use scenarios from baseline period (2010)

	2010					
Land-use types	**(Area, km²)**	**Ratio (%)**	**SL1 Ratio (%)**	**SL2 Ratio (%)**	**SL3 Ratio (%)**	**SL4 Ratio (%)**
FRST	48,002.73	48.73	14.27	0	(−48.73)	0
PAST	26,294.19	26.69	0	14.27	48.73	(−26.69)
WATR	868.64	0.88	0	0	0	0
URBN	951.01	0.97	0	0	0	0
PALD	69.27	0.07	0	0	0	0
PADY	8,258.65	8.38	0	0	0	0
AGRL	14,055.52	14.27	(−14.27)	(−14.27)	0	26.69

Changes in annual runoff

Compared to the simulation results (Table 7) of 2010 land-use type (Figure 3, baseline land cover), the mean annual surface runoff under the SL3 scenario reached a maximum value of 196 mm. Then, the increase in cultivated land resulted in an increase of 192.4 mm (SL4) in surface runoff and also increased for the conversion of cultivated land to forestland (177.5 mm) and grassland (182.4 mm). Similarly, the decrease in cultivated land (SL2) and the increase in forestland (SL1) contributed positively to water yield (520.3 mm for the SL1 scenario and 496.7 mm for the SL2 scenario), and the disappearance of forestland (SL3) or grassland (SL4) reduced water yield, compared to the land-use types of 2010. Meanwhile, an increase in evaporation was also observed when the vegetation rate increased (SL1 to SL3), such as the transformation among cultivated land, forestland, and grassland. Conversely, evaporation decreased to 575.7 mm when grassland was replaced by cultivated land (SL4). At the same time, the conservation index and runoff change rate were 0.225 and 10.02% for the SL1 scenario and 0.208 and 5.03% for the SL2 scenario, respectively. These values were largely affected by vegetation types, i.e., the SL2 scenario forestland and grassland. Runoff decreased 4.96% and 7.97% under the

Table 7 | Hydrological elements under the four land-use scenarios

Land-use scenarios	Surface runoff (mm)	Water yield (mm)	Evaporation (mm)	Conservation index	Runoff change rate (%)
SL1	177.5	520.3	595.4	0.225	10.02
SL2	182.4	496.7	600.2	0.208	5.03
SL3	196.0	449.4	605.1	0.165	−4.96
SL4	192.4	435.2	575.7	0.196	−7.97
2010	162.8	473.5	586.3	0.193	/

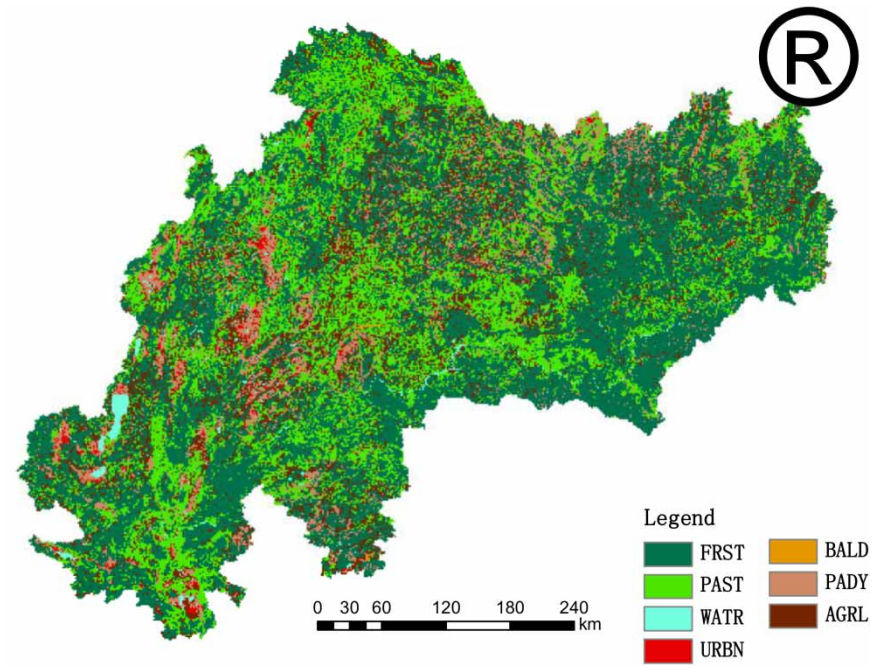

Figure 3 | Land-use type of 2010 in the Longtan basin.

SL3 and SL4 scenarios, respectively, which may have been due to the decreases in forestland and grassland.

Changes in monthly runoff

Monthly runoff variation under the four land-use scenarios (Table 8) demonstrated that dry season runoff (November to April) under the SL1 scenario ranked first, with a maximum value of 18.9 mm, followed by the SL2 and SL4 scenarios, and the SL3 scenario had the lowest monthly flow with a minimum value of 8.1 mm. In contrast, runoff under the SL3 scenario had the greatest surface discharge in the flood season, reaching a maximum value of 187.9 mm and the SL1 scenario produced the minimum surface runoff (merely 158.7 mm).

DISCUSSION

Uncertainties in runoff simulation

The simulation results for different climate and land-use change scenarios had great uncertainties, as did model calibration and validation. However, sensitivity ranking of the parameters CN_2, ALPHA_BF, GW_DELAY, GWQMN, and GW_REVAP was consistent with the results of other studies in similar catchments (Lv *et al.* 2014; Yang *et al.* 2017; Huang *et al.* 2018). On the other hand, although agreement between monthly observations and simulations was achieved, peak discharge for dry months was not a good fit and was underestimated before 2002 or overestimated after 2002. This outcome may have resulted from the construction of the Longtan hydropower dam, which further influenced the condition of the underlying surface. Alternatively, the peak mismatch can be attributed to CN_2, which assumed a unique relationship between cumulative rainfall and runoff in the same antecedent moisture conditions (Khoi & Suetsugi 2014). However, the objective of this study was not to predict floods. Therefore, this mismatch in peak flow can be ignored in this paper.

Table 8 | Monthly average surface runoff under the four land-use scenarios

	Month	SL1	SL2	SL3	SL4
Surface runoff in dry seasons (mm)	11	4.8	4.0	2.8	4.0
	12	3.1	2.1	0.6	1.5
	1	2.6	1.7	0.1	1.0
	2	2.6	2.1	0.6	1.4
	3	3.1	2.6	1.3	2.1
	4	2.7	2.3	2.7	3.1
	Sum	18.9	14.8	8.1	13.1
Surface runoff in rainy seasons (mm)	5	15.5	16.4	18.7	18.5
	6	49.6	52.2	57.3	56.4
	7	43.6	46.1	51.5	48.6
	8	26.7	28.4	32.4	29.8
	9	15.6	16.4	18.7	18.5
	10	7.7	8.2	9.4	7.5
	Sum	158.7	167.6	187.9	179.3

Sensitivity to climate change

For the maximum variations in runoff and evaporation due to climate change in the section 'Sensitivity analysis under climat change', the mean annual runoff and evaporation decreased by 199.5 mm (173.5 mm) and 16.7 mm (41 mm) when temperature increased (decreased) by 1 °C to 2 °C and rainfall decreased by 20%; values increased by 182.1 mm (214.6 mm) for runoff and 33 mm (2.4 mm) for evaporation when temperature increased (decreased) by 1 °C to 2 °C and rainfall increased by 20% on average. Similar results can be obtained from Kong & Liang (2007), Wang *et al.* (2010), and Xu *et al.* (2018), who all indicated a high relation coefficient between rainfall and runoff. This study illustrated that in a karstic basin (Huang *et al.* 2017), rainfall directly infiltrated underground because of the development of surface rock cracks, fissures, and underground channels. Then rainfall further flowed elsewhere and gathered at the surface. The structure of poor storage capacity in karstic fissures was the major reason for the high correlation between precipitation and runoff. However, evaporation was small in the underground karst environment due to the shallow soil layer and high infiltration (Peng & Wang 2012). This situation may further lead to a relatively small impact on runoff variation when temperature increased. Based on the possible runoff response to rainfall and temperature change, reservoir managers can restore more water on poor rainy days, or release more rain water on rainy days.

Sensitivity to land-use change

Runoff responses to the four land-use scenarios were generally in agreement with the research literature, with some

differences. For the annual time scale, deforestation and plantation (SL1 and SL2 scenarios) usually increased evapotranspiration, leading to less runoff (D'Almeida *et al.* 2010). Conversely, deforestation and urbanization (SL3 and SL4 scenarios) decreased evaporation and led to increased runoff (Dunkell *et al.* 2011). Relevant studies (Huang *et al.* 2012) have shown that damage to surface vegetation impaired rain water interception, collection, and holding capacity, and further increased surface discharge. Therefore, the decrease in forest coverage in the SL3 scenario (runoff reached 196.0 mm) would lead to serious soil and water losses in the study area. Regarding the response of monthly runoff to the four land-use scenarios, increased forest cover (SL1 and SL2 scenarios) clearly led to reduced floods, and reduced forest cover caused increased floods (Sahin & Hall 1996). Hence, during the rainy seasons, the conversion to forestland or grassland could prolong the infiltration process of surface runoff and effectively increase the soil water content. Meanwhile, the prolonged infiltration process can store the excess precipitation to recharge for water shortages in the dry season, and finally increase the available water resources and alleviate the drought effect. Obviously, high vegetation coverage under the SL1 scenario could greatly reduce surface runoff and weaken peak discharge during the flood season, which could avoid or alleviate flood disasters, to some extent. According to the runoff sensitivity to land-use scenarios, the reservoir planner should continue to address the measures of conversion of cropland to forest and grassland in western China. Particular attention should be paid to improving land cover to make a relative steady runoff change process.

CONCLUSIONS

This paper focuses on sensitivity analysis of runoff to climate and land-use changes, which is vital to provide deeper and better technical support for the watershed management and making ecology strategies. The main innovations include: (1) Constructing climate and land-use change scenarios based on the major impact factors for runoff variability, in the karstic area. (2) Simulating the hydrological process under different scenarios of climate and land-use change at different scales (annual and monthly). (3) Identifying the major impact factors for runoff variability based on quantitative analysis via the research approach of 'climate scenarios-hydrological simulation-response analysis'.

The results of this study will be useful for understanding the potential impact of climate and land-use changes on runoff for similar catchments and meet the strong demand for proper measures aimed at global warming adaptation and soil and water conservation and protection.

ACKNOWLEDGEMENTS

The authors would like to thank the National Natural Science Foundation of China (Grant No. 51569003), the Natural Science Foundation of Guangxi Province (Grant No. 2017GXNSFAA198361) and the Innovation project of Guangxi Graduate Education (Grant No. YCBZ2018023).

SUPPLEMENTARY MATERIAL

The Supplementary Material for this paper is available online at https://dx.doi.org/10.2166/wcc.2020.196.

REFERENCES

Abbaspour, K. C., Yang, J., Maximov, I., Siber, R., Bogner, K., Mieleitner, J., Zobrist, J. & Srinivasan, R. 2007 Modelling hydrology and water quality in the pre-alpine/alpine Thur watershed using SWAT. *Journal of Hydrology* **333** (2), 413–430.

Arnold, J. G. 2012 SWAT: model use, calibration, and validation. *Transactions of the ASABE* **55** (4), 1491–1508.

Arnold, J. G., Srinivasan, R., Muttiah, R. S. & Williams, J. R. 1998 Large area hydrologic modeling and assessment part I: model decelopment. *JAWRA Journal of the American Water Resources Association* **34** (1), 91–101.

Chen, H., Xu, C. & Guo, S. 2012 Comparison and evaluation of multiple GCMs, statistical downscaling and hydrological models in the study of climate change impacts on runoff. *Journal of Hydrology* **434–435**, 36–45.

Chenoweth, J., Hadjinicolaou, P., Bruggeman, A., Lelieveld, J., Levin, Z., Lange, M. A., Xoplaki, E. & Hadjikakou, M. 2011 Impact of climate change on the water resources of the eastern Mediterranean and Middle East region: modeled 21st century changes and implications. *Water Resources Research* **47** (6), W06506+.

Chesworth, W., Arbestain, M. C., Macías, F., Spaargaren, O., Spaargaren, O., Mualem, Y., Morel Seytoux, H. J., Horwath, W. R., Almendros, G. & Chesworth, W. 2008 Classification of soils: FAO. In: *Encyclopedia of Soil Science* (W. Chesworth, ed.). Springer, Doerdrecht, the Netherlands, pp. 111–113.

D'Almeida, C., Vörösmarty, C. J., Hurtt, G. C., Marengo, J. A., Dingman, S. L. & Keim, B. D. 2010 The effects of deforestation on the hydrological cycle in Amazonia: a review on scale and resolution. *International Journal of Climatology* **27** (5), 633–647.

Dittmer, K. 2013 Changing streamflow on Columbia basin tribal lands – climate change and salmon. *Climatic Change* **120** (3), 627–641.

Dunkell, D. O., Bruland, G. L., Evensen, C. I. & Litton, C. M. 2011 Runoff, sediment transport, and effects of feral pig (Sus scrofa) exclusion in a forested Hawaiian watershed. *Pacific Science* **65** (2), 175–194.

Ghoraba, S. M. 2015 Hydrological modeling of the Simly Dam watershed (Pakistan) using GIS and SWAT model. *Alexandria Engineering Journal* **54** (3), 583–594.

Green, T. R., Taniguchi, M. & Kooi, H. 2007 Potential impacts of climate change and human activity on subsurface water resources. *Vadose Zone Journal* **6** (3), 531–532.

Gusev, Y. M., Nasonova, O. N., Kovalev, E. E. & Ayzel, G. V. 2018 Impact of possible climate changes on river runoff under different natural conditions. *Proceedings of the International Association of Hydrological Sciences* **379**, 293–300.

Huang, C. B., Tan, W. N., Qin, W. G., Wei, G. F., Min, W. U. & Wei, Y. L. 2012 Study on soil and water loss in karst forest in Mulun. *Research of Soil & Water Conservation* **19** (4), 34–37.

Huang, Y., Xiao, W. & Chen, L. 2017 Analysis of temperature and precipitation characteristics in Longtan Reservoir Basin during 1959–2014. *Water Power* **2**, 18–22.

Huang, F. H., Huang, B. S., Qiu, J., Zhao, J. G. & Liu, D. 2018 Simulative study on impact of climate change on runoff within Beijiang River basin. *Water Resources and Hydropower Engineering* **49** (1), 23–28.

Jiang, Z., Chen, W. & Li, L. 2015 Probabilistic projections of climate change over China under the SRES A1B scenario using 28 AOGCMs. *Journal of Climate* **24** (17), 4741–4756.

Jones, R. N., Chiew, F. H. S., Boughton, W. C. & Zhang, L. 2006 Estimating the sensitivity of mean annual runoff to climate change using selected hydrological models. *Advances in Water Resources* **29** (10), 1419–1429.

Khoi, D. N. & Suetsugi, T. 2014 Impact of climate and land-use changes on hydrological processes and sediment yield-a case study of the Be River catchment, Vietnam. *International Association of Scientific Hydrology Bulletin* **59** (5), 1095–1108.

Kim, S., Kim, B. S., Jun, H. & Kim, H. S. 2014 Assessment of future water resources and water scarcity considering the factors of climate change and social–environmental change in Han River basin, Korea. *Stochastic Environmental Research & Risk Assessment* **28** (8), 1999–2014.

Kong, L. & Liang, H. 2007 Analysis to runoff evolution features along time series in karst drainage basin – A case study in Guizhou province. *Carsologica Sinica* **26** (4), 341–346.

Li, S. D. 2002 Policies of conversion of cropland to forest and grassland in middle and western China. *Journal of Beijing Forestry University (Social Science)* **1** (1), 11–17.

Li, S. D. & Wu, Z. Y. 2002 Study on models of conversion of cropland to forest and grassland in the Midwest China. *Scientia Silvae Sinicae* **3** (38), 155–159.

Liston, G. E. & Elder, K. 2006 A meteorological distribution system for high-resolution terrestrial modeling (MicroMet). *Journal of Hydrometeorology* **7** (2), 217–234.

Lv, L. T., Peng, Q. Z., Guo, Y. Y., Liu, Y. H. & Jiang, Y. 2014 Runoff simulation of Dongjiang River basin based on the soil and water assessment tool. *Journal of Natural Resources* **10**, 1746–1757.

Miller, N. L. 2005 Local climate sensitivity of the Three Gorges Dam. *Geophysical Research Letters* **32** (16), 1–12.

Mo, G. Y. 2018 *Runoff Response to the Climate and Land-use Change in the Longtan Basin*. Guangxi University, Nanning, Guangxi, China.

Moriasi, D. N., Arnold, J. G., Liew, M. W. V., Bingner, R. L., Harmel, R. D. & Veith, T. L. 2007 Model evaluation guidelines for systematic quantification of accuracy in watershed simulations. *Transactions of the ASABE* **50** (3), 885–900.

Peng, T. & Wang, S. J. 2012 Effects of land use, land cover and rainfall regimes on the surface runoff and soil loss on karst slopes in southwest China. *Catena* **90** (1), 53–62.

Pizzolotto, R. & Brandmayr, P. 1996 An index to evaluate landscape conservation state based on land-use pattern analysis and Geographic Information System techniques. *Coenoses* **11**, 37–44.

Sahin, V. & Hall, M. J. 1996 The effects of afforestation and deforestation on water yields. *Journal of Hydrology* **178** (1–4), 293–309.

Şen, Z. 2009 Global warming threat on water resources and environment: a review. *Environmental Geology* **57** (2), 321–329.

Shi, W. H. 2014 *Research on Flood Season Staging and Adjustment of Limited Water Level on Longtan Basin*. Guangxi University, Nanning, Guangxi, China.

Silberstein, R. P., Aryal, S. K., Durrant, J., Pearcey, M., Braccia, M., Charles, S. P., Boniecka, L., Hodgson, G. A., Bari, M. A. & Viney, N. R. 2012 Climate change and runoff in south-western Australia. *Journal of Hydrology* **475** (12), 441–455.

Somura, H., Arnold, J., Hoffman, D., Takeda, I., Mori, Y. & Luzio, M. D. 2009 Impact of climate change on the Hii River basin and salinity in Lake Shinji: a case study using the SWAT model and a regression curve. *Hydrological Processes* **23** (13), 1887–1900.

Wang, S., Kang, S., Zhang, L. & Li, F. 2010 Modelling hydrological response to different land-use and climate change scenarios in the Zamu River basin of northwest China. *Hydrological Processes* **22** (14), 2502–2510.

Wang, G., Yang, H., Wang, L., Xu, Z. & Xue, B. 2014 Using the SWAT model to assess impacts of land use changes on runoff

generation in headwaters. *Hydrological Processes* **28** (3), 1032–1042.

Wu, P. & Tan, M. 2012 Challenges for sustainable urbanization: a case study of water shortage and water environment changes in Shandong, China. *Procedia Environmental Sciences* **13** (3), 919–927.

Wu, L., Wang, S., Bai, X., Luo, W., Tian, Y., Zeng, C., Luo, G. & He, S. 2017 Quantitative assessment of the impacts of climate change and human activities on runoff change in a typical karst watershed, SW China. *Science of the Total Environment* **601–602**, 1449–1465.

Xu, Y., Wang, S., Bai, X., Shu, D. & Tian, Y. 2018 Runoff response to climate change and human activities in a typical karst watershed, SW China. *Plos One* **13** (3), e0193073.

Yan, R., Cai, Y., Li, C., Wang, X. & Liu, Q. 2019 Hydrological responses to climate and land use changes in a watershed of the Loess Plateau, China. *Sustainability* **11** (5), 1443.

Yang, M. Z., Xiao, W. H., Lu, F., Huang, Y., Hou, B. D. & Li, X. D. 2017 Impact of climate change on water resource in coastal areas of South China. *Journal of Guangxi University (Natural Science Edition)* **42** (5), 1951–1959.

Zhou, B., Wen, Q. H., Xu, Y., Song, L. & Zhang, X. 2014 Projected changes in temperature and precipitation extremes in China by the CMIP5 multimodel ensembles. *Journal of Climate* **27** (17), 6591–6611.

Zhou, Y., Shi, C., Fan, X. & Shao, W. 2015 The influence of climate change and anthropogenic activities on annual runoff of Huangfuchuan basin in northwest China. *Theoretical & Applied Climatology* **120** (1–2), 137–146.

First received 3 September 2019; accepted in revised form 23 February 2020. Available online 10 November 2020